

A NODE ANTENNA DESIGN WITH COSECANT SQUARED BEAM

J. R. BERGMANN

CATHOLIC UNIVERSITY OF RIO DE JANEIRO - CETUC
 Rua Marquês de São Vicente, 225 - 22453 - RJ - BRAZIL

Abstract. This paper presents a design for a reflector antenna that illuminates a large sector of the space with cosecant squared vertical pattern. The configuration considered is composed of a shaped reflector fed by a corrugated conical horn. The reflector shape is obtained by Geometrical Optics principles. The radiation pattern obtained by a diffractive analysis shows good agreement with the specifications.

1. INTRODUCTION

A broadcasting antenna for point-to-multipoint transmission in a metropolitan area must provide uniform coverage, requiring a vertical pattern in the form $G(\alpha) = [\Lambda/\sin^2(\alpha)]$ (see Fig. 1) in order to compensate the power dependence ($1/R^2$) on the distance R to the node. The omnidirectional azimuth radiation is obtained by an arrangement of wide beam antennas each covering a sector of space. This pattern beam has been synthesised by designs that employ arrays, slot antennas, beam horns and shaped reflectors [1-5].

The option considered for study herein is composed of a shaped reflector illuminated by a single feed. For this configuration, Koch and Thielen [4] obtained the reflector shaping by employing a technique based on a diffractive analysis associated with optimisation methods. Despite the satisfactory results, this technique is highly demanding on computer time, specially when large areas have to be covered. Alternatively, Geometrical Optics (GO) principles can be used to obtain the reflector profile with substantial reduction in the computational effort. For an arbitrary farfield, Norris and Westcott [6] have formulated a reflector synthesis method, under GO assumptions, as a boundary value problem. As diffraction is ignored, this GO technique shows limitations to control the radiation outside the main coverage zone or to obtain focused beams. In this work, we explore the application of this synthesis method [6] to design a node antennas for point-to-area coverage which has a narrow beam in the vertical plane and a broad one in the azimuthal plane.

2. FARFIELD SPECIFICATION

The polygon-reflector antenna chosen for design is composed of four shaped reflectors arranged in form of a square, each of them having one horn radiator as feed. Thus, each of the shaped reflectors has to illuminate a quadrant of the space.

By using α and β defined in Fig. 1, the radiation pattern can be described by separable functions $G(\alpha, \beta) = G_1(\alpha)G_2(\beta)$ as shown in Fig. 2. The evaluation pattern $G_1(\alpha)$ is a pencil beam with 6° full 3dB beamwidth having a cosecant squared roll off below horizon starting at -3° and continuing over to 45° , while, the azimuthal pattern $G_2(\beta)$ is constant over the quadrant $|\beta| < 45^\circ$. The specifications allow discrepancies of ± 3 dB. For the synthesis, the vertical pattern between $\pm 3^\circ$ has been modelled by the function $\exp[-a \cdot \sin^2(\alpha)]$.

3. FEED MODEL

The feed considered for the design is a 90° corrugated horn with a 3

wavelengths (λ) aperture diameter. Fig. 3 shows the measured patterns in the E and H planes.

The phase measurement of the feed is represented by $\Delta\psi$ which is the phase deviation from a spherical phase front referred to the phase center. By using these plane cuts, the power density radiation by the feed is given by $I[\theta', \phi'] = [I_H(\theta') \cos^2 \phi' + I_E(\theta') \sin^2 \phi']$ where θ' and ϕ' are referred to the feed axis. For the synthesis and analysis computations, the power density on the principal planes of polarisation, I_E and I_H have been modelled by analytical functions that compare well the measurements.

4. CONFIGURATIONS

The ray configuration chosen is a top to bottom design where a feed ray incident on the top of reflector is reflected to the bottom ($\alpha = 75^\circ$) of the farfield pattern as shown in the Fig. 4. This configuration have a caustic surface in front the reflector. It has the advantage of allowing the offset angle θ_0 to be adjusted for no feed blockage. It also places the feed below the reflector which requires a simple cabling. In order to fairly approximate this cosecant pattern with a sharp peak, the vertical dimension was designed to have a 40λ (about 115 cm).

5. REFLECTOR SHAPE

The full details of the reflector synthesis procedure adopted can be found in Westcott [7] and we shall merely state the main results. This formulation employs the complex coordinates η and ξ to represent the directions of the incident and reflected rays (Fig. 5), respectively. The reflector surface is described by a function $L(\eta, \bar{\eta})$ which is associated to $r(\eta)$ by $L = r/(1+|\eta|^2)$. The complex conjugate of η is represented by $\bar{\eta}$. This choice results in a simple expression for the Snell's Law of reflection $\xi = \eta + 1/L_\eta$ where L_η is the partial derivative with respect to η . The energy relation between the primary pattern $I(\eta)$ radiated by a source-point the secondary pattern $G(\xi)$ is given by the following differential equation

$$|L_{\eta\eta} - L_\eta^2| - L_{\eta\bar{\eta}}^2 = |L_\eta|^4 \frac{[1+|\eta|^2]^2 I(\eta)}{[1+|\xi|^2]^2 G(\xi)}$$

resulting from applying energy conservation on a tube of rays. This partial differential equation is of the Monge-Ampere type and its elliptic form was considered. Solution of the above equation will yield the function $L(\eta, \bar{\eta})$, and the position vector of the points on the reflector then follows from the equation $\vec{r} = e^L[(\eta, \bar{\eta}), i(\bar{\eta}, \eta), (|\eta|^2 - 1)]$.

Boundary Condition

The Monge-Ampere equation is solved under a boundary condition which enforces a 1:1 mapping between rays at the edge cone source and the rays at the edge of the farfield boundary. The incident illumination from the source-point is assumed to exist within a cone of semi-vertex angle $\theta_c = 45^\circ$. The feed boresight direction coincides with the cone axis and is tilted of $\theta_0 = 50^\circ$ with the z-axis.

The farfield region considered for synthesis is defined by $3^\circ < \alpha < 45^\circ$ and $|\beta| < 45^\circ$. Outside this area, the GO synthesis shows limitations in controlling low levels of energy since, there, the diffractive effects are dominant.

Numerical Solution

By defining a regular polar grid of points with center at the feed axis, nu-

merical solutions were obtained by applying a finite difference scheme to the Monge-Ampere equation and its boundary condition[7]. It results in a system of non-linear algebraic equations which are then solved using a generalization of Newton's technique. The whole iterative algorithm is well documented in Westcott [6].

The solution chosen to initialize the iterative procedure was obtained from the analytical expression for a hyperboloid which transforms the circular cone θ_c into a circular region on the farfield. Convergence of the iterative procedure was then obtained by the slow and continuous deformation of the boundary condition.

5. ANALYSIS AND COMMENTS

The synthesised reflector surface is described by a set of points which are fitted by surface models in order to obtain a continuous representation. A diffractive analysis was then performed by integrating the Physical Optics currents on the reflector surface. Fig.6 shows the power pattern obtained on several ϕ -planes and a comparison with the specifications. Although the synthesis formulation considers a source point illuminating the reflector, the analysis includes the phase deviation $\Delta\psi$ in the feed model.

Despite the ripples introduced by diffraction, its most significant effects were observed on the plane cuts close to the horizontal plane. There, diffraction has rounded the patterns shape reducing the -3. dB beamwidth. To compensate this effect, $G(\alpha)$ was extended to 47° and multiplied by a gaussian $[\exp(c\beta^2)]$ where c was chosen for a 2dB increase in the edge illumination.

Due to the symmetry, the crosspolarisation is null along the plane $\phi=0^\circ$. A peak of -17. dB was found along the horizontal plane (asymmetry plane). As the feed crosspolarisation peak is below -30. dB, the depolarisation effects are dominated by the shaping. Reductions in the crosspolar component can be obtained by using feed patterns with a narrower beam that permits to reduce the offset angle. However, the use of smaller θ_c generates less compact designs.

REFERENCES

1. Ashton, R.W.: "The Martello 3D Radar Antenna", IEE-Conference Publication 169, Pt.1, (1978).
2. Nash, J.R.: "Slot array antenna having a complex impedance termination and method of fabrication", United States Patent Application, N258411, July, 1979.
3. Sha, K., Kakata, W., Adachi, S.: "Design of E-plane Cosecant Square Beam Horn Antennas Based on Ray Theory and Their Radiation Characteristic", Trans. IECE, Japan, Vol. 64-B, No 5, 1981, pp. 100-107.
4. Koch, G., and Thielen, H.: "Transmitting Antenna with Cosecant-Shaped Vertical Pattern for the 12-GHz Television System", IEEE Trans. on Communications, Vol. COM-22, No9, September, 1974.
5. Dunbar, A.S.: "Calculation of doubly curved reflectors for shaped beams", Proc. IRE, 1948, 36, pp. 1289-1296.
6. Norria, A.P., and Westcott, B.S.: "Computation of reflector surfaces of bivariate beamshaping in the elliptic case", J. Phys., A, 1976, pp. 2159-2169.
7. Westcott, B.S.: "Shaped reflector antenna design", (Research Studies Press, Lechworth, Herts, 1983).

This work was supported by TELEBRÁS under contract PUC/TELEBRÁS-168/83.

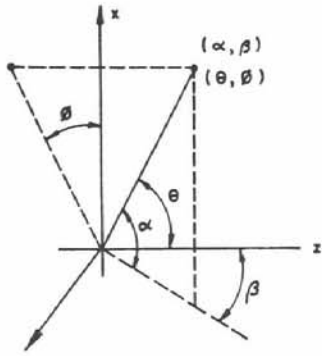


FIG. 1 - SYSTEMS OF COORDINATE

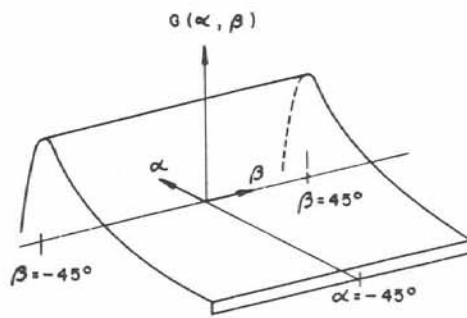


FIG. 2 - DESIRED POWER PATTERN

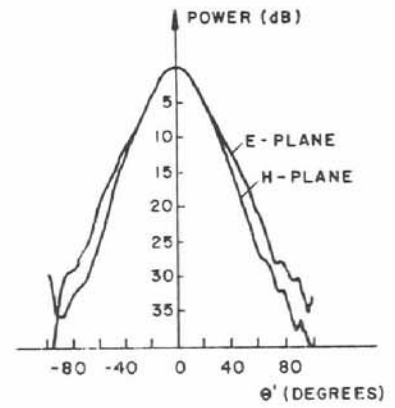


FIG. 3 - MEASURED FEED POWER PATTERN

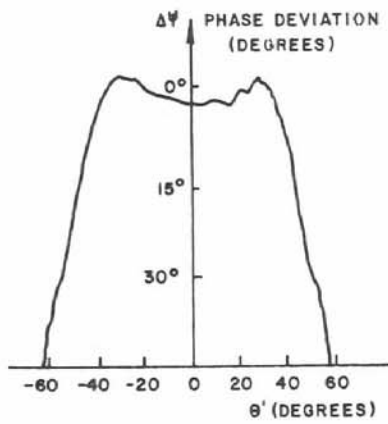


FIG. 3.b - MEASURED PHASE DEVIATION

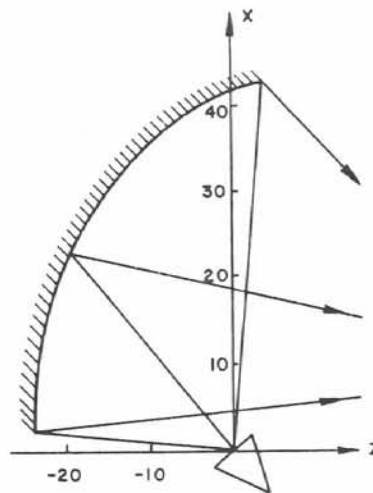


FIG. 4 - RAY GEOMETRY

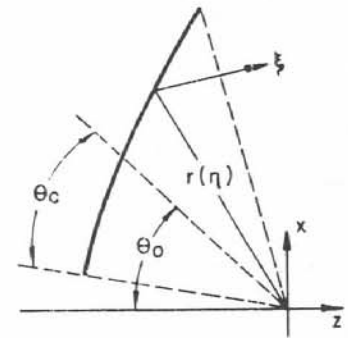


FIG. 5 - SUBREFLECTOR SURFACE

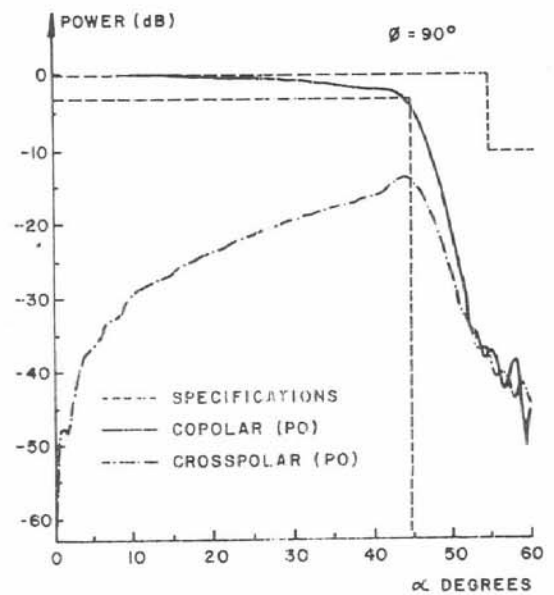
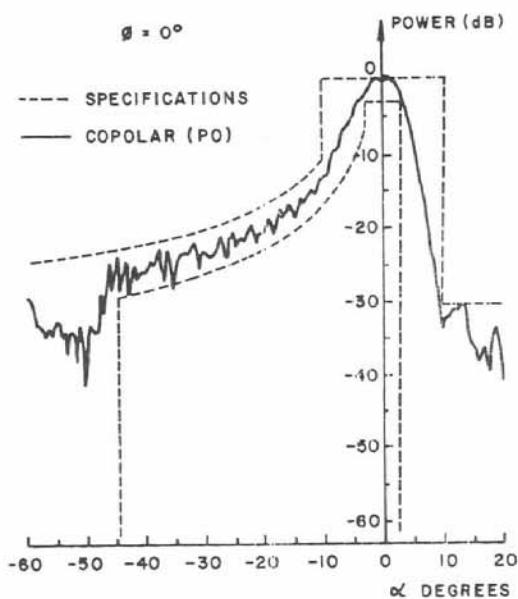


FIG. 6 - POWER PATTERNS OBTAINED FROM PO ANALYSIS